Dynamic Spin-Polarized Resonant Tunneling in Magnetic Tunnel Junctions

Casey W. Miller,[1,*] Zhi-Pan Li,[1,†] Ivan K. Schuller,[1] R. W. Dave,[2] J. M. Slaughter,[2] and Johan Åkerman[3]

[1]*Department of Physics, University of California, San Diego, 9500 Gilman Drive, La Jolla, California 92093, USA*

[2]*Technology Solutions Organization, Freescale Semiconductor, Inc., 1300 North Alma School Road, Chandler, Arizona 85224, USA*

[3]*Department of Microelectronics and Applied Physics, Royal Institute of Technology, Electrum 229, 164 40 Kista, Sweden*

(Received 26 February 2007; published 27 July 2007)

Precisely engineered tunnel junctions exhibit a long sought effect that occurs when the energy of the electron is comparable to the potential energy of the tunneling barrier. The resistance of metal-insulator-metal tunnel junctions oscillates with an applied voltage when electrons that tunnel directly into the barrier's conduction band interfere upon reflection at the classical turning points: the insulator-metal interface and the dynamic point where the incident electron energy equals the potential barrier inside the insulator. A model of tunneling between free electron bands using the exact solution of the Schrödinger equation for a trapezoidal tunnel barrier qualitatively agrees with experiment.

DOI: 10.1103/PhysRevLett.99.047206 PACS numbers: 85.75.−d, 72.25.−b, 75.70.−i

Tunneling through a barrier is one of the most fundamental problems in physics with profound technological implications [1–5]. Electron tunneling can be realized in multilayer systems consisting of two conducting electrodes separated by an insulating material. These tunneling devices can have electrodes that are normal metals (e.g., Au), superconductors (Al), or ferromagnets (Fe), while the insulators range from semiconductors (Ge) to metal oxides (MgO). In all cases, the energy difference between the Fermi energy of the electrodes and the conduction band of the barrier defines the height of the tunneling barrier. The relative energy of the tunneling electrons is varied by applying a voltage bias between the electrodes. The barrier material's properties generally play no role because the barrier potential is typically much greater than the energy of the tunneling electron. However, recent technological advances have led to robust oxide barriers that can withstand large electric fields, which allows access to electrons with energies comparable to the barrier potential. It was predicted long ago that a tunneling electron could access electronic states in the barrier and undergo resonant tunneling [6], though this has not been directly observed in metal-insulator-metal junctions with a single tunnel barrier. This Letter reports well-defined and reproducible bias-dependent oscillations of the differential resistance in CoFeB/MgO/NiFe tunnel junctions that are consistent with interfering electrons within the MgO barrier. Further, we are able to use the ferromagnetism of the electrodes to investigate these oscillations in terms of a tunneling magnetoresistance. Qualitative agreement with these data is obtained using a simple tunneling model where the electrodes are treated as free electron bands and the tunneling matrix elements are determined by solving the Schrödinger equation exactly for a trapezoidal barrier.

The procedure used to fabricate our magnetic tunnel junctions (MTJs) was reported previously [7]. We investigated about 30 MTJs each of CoFeB/MgO/NiFe (NiFe) and two sets of CoFeB/MgO/CoFeB (CFB1 and CFB2), for a total of nearly 90 junctions. As-deposited CoFeB is amorphous, while NiFe is polycrystalline. The barriers were formed by oxidizing 16 Å of Mg, which should produce a 13 Å thick MgO barrier. All devices were fabricated identically with the exceptions of the free layer material and the procedure for oxidation and annealing. While data presented here are for 1 μm^2 MTJs, our observations were independent of device shape and area, which varied from 1100 nm $\times$ 420 nm ellipses to 600 nm–10 μm diameter circles; heating and series resistances were thus negligible. The temperature dependence can be attributed to thermal smearing [8], and all devices satisfied the MTJ tunneling criteria [9,10], proving that tunneling is the primary conduction mechanism.

Direct measurements of the differential resistance (dV/dI) were made with the magnetizations of the ferromagnets (in remanence) in parallel (p) and antiparallel (ap) configurations using a high resolution ac resistance bridge and standard lock-in techniques. The dc bias was applied to the free layer (NiFe or CoFeB) with the pinned layer (CoFeB) grounded. Figure 1 shows dV/dI measurements of a NiFe device at 5 K. An obvious oscillation for positive biases is apparent in the ap state; a low amplitude oscillation is also present in the p state. The dV/dI evolve continuously between these states as a function of the angle between the free and pinned magnetizations. dV/dI_p equals dV/dI_{ap} at several biases, the highest of which (+1.8 V) was observable at 5 K because of an increase in the breakdown voltage at low temperatures. These crossing biases were independent of temperature and the relative orientation of the ferromagnets.

Though the underlying physics is contained in the dV/dI for each magnetic orientation, inspecting the differential junction magnetoresistance (dMR) is a convenient way to emphasize this oscillatory behavior. Defining the dMR as

$$\mathrm{dMR} = \frac{dV/dI_{ap} - dV/dI_p}{dV/dI_p},$$

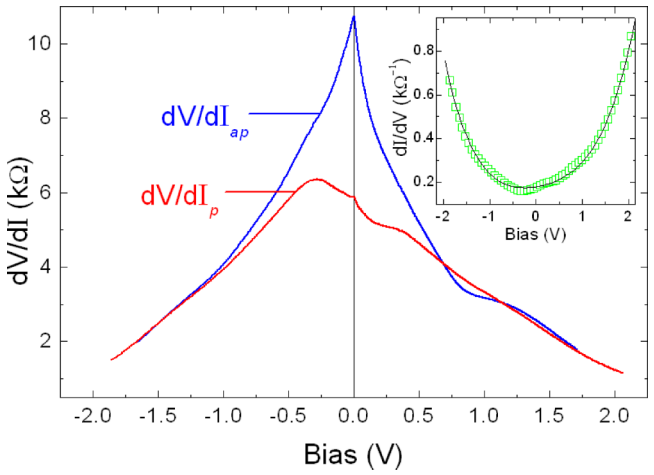

FIG. 1 (color online). Differential resistance measurements of NiFe devices at 5 K in the p and ap magnetic configurations. (inset) The bias dependence of dI_p/dV for NiFe (green squares) is fit well by a 4th order polynomial (black line).

it is most common to observe dMR > 0 because the density of states bottleneck typically causes dV/dI_{ap} to exceed dV/dI_p. Thus, the most striking feature of Fig. 2 is that the dMR of the NiFe devices oscillates about zero when electrons tunnel from CoFeB into NiFe. In contrast, no oscillations were observed for either CFB1 or CFB2 (though these did have dMR < 0 at high biases). The symmetry of the biases for which dMR initially changes sign (i.e., the first zero crossings for both polarities) mimics that of the barrier shape. The barrier parameters extracted using the Brinkman, Dynes, and Rowell (BDR) model [11]

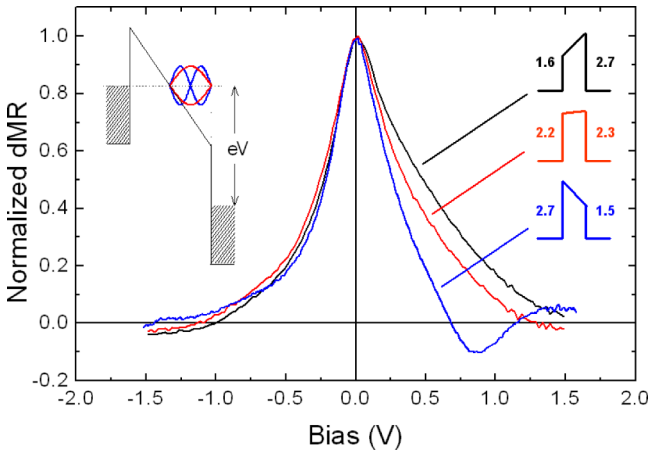

FIG. 2 (color online). Normalized differential magnetoresistance for NiFe (bottom, blue), CFB1 (middle, red), and CFB2 (top, black) at 300 K. The nominal dMR ($V = 0$) and resistance-area products were 80% and 3.1 k$\Omega \cdot \mu$m^2 for NiFe, and 120% and 6.0 k$\Omega \cdot \mu$m^2 for both CFB devices. The barrier heights (eV) from BDR fits of dI_p/dV are indicated schematically to the right, and a cartoon of electron standing waves is shown to the left.

for each device type are shown schematically in Fig. 2. CFB1 had a relatively symmetric barrier and symmetric zero crossings. The first zero crossing for NiFe occurs when electrons tunnel toward the low barrier interface. CFB2 had the opposite symmetry of the NiFe devices both in barrier heights and zero crossings. Based on this seemingly general behavior, we predict similar oscillations would be seen for both polarities in NiFe/MgO/NiFe devices.

One possible explanation for this behavior is dynamic resonant tunneling mediated by electron interference, a result of Fowler-Nordheim (FN) tunneling [12]. In the FN regime, the incident electron energy exceeds the potential near the collector *within the barrier*, which implies that electrons tunnel directly into the MgO conduction band (see cartoon in Fig. 2). These electrons can thus be treated as plane waves near the collector interface. Incident and reflected electrons may then interfere and establish standing waves within this region of the barrier (where the kinetic energy of the electron is real). The maximum oscillation amplitude exists in the ap state, which is the result of spin-dependent reflection from the MgO-NiFe interface. Spin-up electrons tunneling from the CoFeB emitter with positive magnetization toward the NiFe collector with negative magnetization are preferentially reflected at the MgO-NiFe interface because of a spin bottleneck in the density of states. When the applied bias allows for resonant tunneling in the ap state, spin-up emitter electrons dominate the tunneling current. The result of this is that the antiparallel state conductance exceeds that of the parallel state, which leads directly to dMR < 0. Negative dMR indicates that tunneling is dominated by minority-spin electrons rather than majority electrons (as defined in the collector electrode), and oscillations suggest that the relative conductance of the spin species changes with bias. Gundlach showed that oscillations of the conductance (in tunneling between normal metals) can only be described by exactly solving the Schrödinger equation and that this is evidence for the failure of the simplest application of the Wentzel-Kramers-Brillouin (WKB) approximation [6]. This effect has been identified in semiconductor systems [13] and scanning tunneling microscopy [14], but not in metal-insulator-metal heterostructures.

Figure 3 shows that these experimental results are qualitatively reproduced by a model that uses the exact solution of the Schrödinger equation with spin-split free electron bands representing the ferromagnetic electrodes. A free electron model is justified here because tunneling is dominated by s-like electrons [15–17]. This model reproduces the angular dependence of the experimental dMR when the polarization of either electrode is varied as $\cos\theta$, including a nodal behavior of the biases where dMR equals zero (i.e., when $dV/dI_p \equiv dV/dI_{ap}$). Asymmetric barriers were approximated as single-thickness trapezoids with barrier

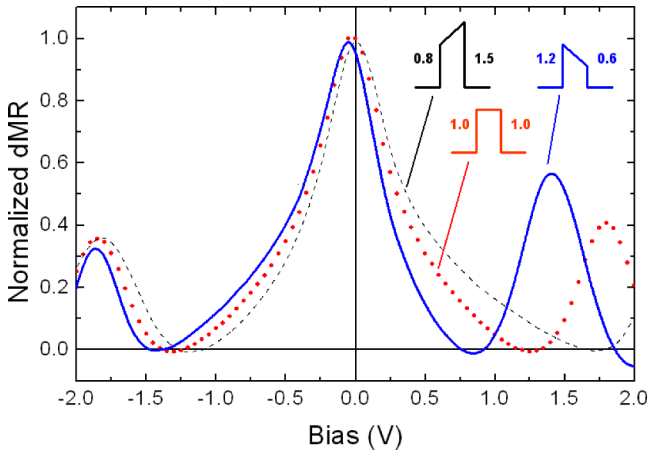

FIG. 3 (color online). Model results for the dMR bias dependence for NiFe (blue line), CFB1 (red dots), and CFB2 (black dashes) show qualitative agreement with experiment. For a thickness of 28 Å and no roughness, the barrier heights (eV) used in the model are indicated schematically to the right.

heights ϕ_1 and ϕ_3 at the pinned and free layer interfaces. We included material-dependent effective masses and thus implemented the BenDaniel-Duke boundary conditions: continuity of the wave function $\psi_i(x_{i,j}) = \psi_j(x_{i,j})$ and flux $\partial_x\psi_i(x_{i,j})/m_i^* = \partial_x\psi_j(x_{i,j})/m_j^*$ at $x_{i,j}$ between materials i and j [18]. Because *ab initio* calculations are unavailable for disordered electrodes, we approximate the (spin-independent) effective masses ($m^* = 1.3m_e$) and band bottoms (2.3 eV below the Fermi energy, E_F) for both electrodes by Fe band structure calculations [19]. The MgO effective mass was taken to be $0.4m_e$ [20]. The spin splittings (Δ) of the electrodes were estimated via $\Delta_i = E_F[(1 - P_i)^2/(1 + P_i)^2 - 1]$, where i denotes the material and the polarizations (P) of CoFeB and NiFe were taken to be 55% and 45% from tunneling spin polarization measurements [21,22]. The tunneling currents in the parallel and antiparallel states were calculated including the spin-dependent densities of states [23] via

$$I_p \propto \int (D_{\uparrow\uparrow}N_\uparrow^{(1)}N_\uparrow^{(3)} + D_{\downarrow\downarrow}N_\downarrow^{(1)}N_\downarrow^{(3)})F(E)dE,$$

$$I_{ap} \propto \int (D_{\uparrow\downarrow}N_\uparrow^{(1)}N_\downarrow^{(3)} + D_{\downarrow\uparrow}N_\downarrow^{(1)}N_\uparrow^{(3)})F(E)dE,$$

where subscripts denote the pertinent spin sub-bands, superscripts denote the materials, and $F(E)$ is the difference in Fermi functions of the two electrodes $[f^{(1)}(E) - f^{(3)}(E - eV)]$. The spin-dependent densities of states for materials 1 (grounded, pinned layer) and 3 (biased free layer) are respectively $N_m^{(1)} = N_m^{(1)}(E)$ and $N_n^{(3)} = N_n^{(3)}(E - eV)$, where subscripts represent the spin sub-bands. The tunneling matrix elements $D_{mn} = D_{mn}(s, \phi_1, \phi_3, V, E)$ are the probabilities of tunneling between spin sub-bands m and n in electrodes 1 and 3, respectively, and they were obtained by exactly solving the Schrödinger equation. Spin-flip processes were neglected. The upper limit of the transverse integration was truncated at 2% of the Fermi energy because the tunneling current is dominated by wave vectors within a cone of ~8° from normal incidence [24]. This model is simple and therefore appealing, though more intricate analyses [25] may capture more effectively the underlying spin-dependent physics.

The location and amplitude of the negative dMR peak shift only slightly when interfacial roughness is included in the calculation in a previously demonstrated manner [26]. This is because the bias of the initial oscillation is set by the barrier height at the collector interface (the threshold bias for FN tunneling equals this height). Note that for CFB1 or CFB2 oscillations were not observed because the barrier heights were comparable to the maximum applied bias. On the other hand, a more significant effect is seen for the positive peak around 1.4 V. Including 15% roughness, which was the roughness determined for similar MTJs [27], causes the amplitude of the latter peak to fall from 58% to 45%, and requires a mean thickness of 35 Å to keep the dMR peaks at biases consistent with the data of Fig. 2; the discrepancy from the growth thickness is reasonable for this qualitative model.

The model needed to explain the present data implies barrier parameters that are different from those obtained by BDR fits. To qualitatively reproduce the data, the model requires similar ϕ_1 with only ϕ_3 significantly different between the three MTJ types (shown schematically in Fig. 3). This is reasonable since the fabrication process for all the devices was identical until the barrier oxidation; perturbations due to this step should predominately affect ϕ_3, not ϕ_1. The BDR fits, on the other hand, indicate a roughly constant average barrier height with both ϕ_1 and ϕ_3 different for each MTJ type, which is less reasonable considering the fabrication procedure. The model calculations use a thickness of 28 Å (when neglecting roughness), while the BDR fits yield ~8 Å. This discrepancy is most likely due to interfacial roughness and the WKB approximation failing in these devices (as indicated by the electron interference presented here).

FN tunneling is required for the interference of electrons within the barrier. In this regime, both the width and average height of the barrier at the Fermi energy decrease with increasing bias. The result of this should be an exponentially increasing conductance for applied biases greater than the collector interface barrier height. The parallel state conductance data are fit well by a fourth-order polynomial (Fig. 1 inset), showing that deviations from the low-bias parabolic behavior exist, but the data are not exponentially increasing at the highest biases. The delayed transition to exponential conductance may be related to the effective mass of the tunneling electron, interfacial roughness, or may be an emerging characteristic of coherent tunneling through crystalline barriers, possibly originating from heating effects [27,28].

Similar oscillations are obtained in resonant tunneling studies where a normal metal spacer exists between the barrier and one ferromagnet (see, e.g., Ref. [29] and references therein). We refer to those as ''static'' phenomena because the thickness of the normal metal is fixed. The phenomenon we report here is ''dynamic'' because the thickness of the interference region can be tuned by the applied bias: electrons inside the MgO conduction band can be treated as free electrons, making this region directly analogous to the normal metal spacer used in static studies. Additionally, the present case allows the effective mass of the MgO conduction band to be estimated from the oscillation period. Recalling that the de Broglie wavelength (in Å) is $\lambda = 0.529\varepsilon m_e/m^*$, where ε is the dielectric constant ($\varepsilon \sim 3$) and m^*/m_e is the reduced mass of MgO [30], the measured oscillation period corresponds to $\lambda \sim 2.6$ Å and $m^* \sim 0.6m_e$, in reasonable agreement with the expected $0.4m_e$ [20].

Alternate explanations for our observations can be ruled out. The oscillations are odd functions of bias and thus cannot be explained by emission phenomena such as magnons [31]. The persistence of the oscillatory nature at finite bias with interface roughness excludes localized barrier states and interface resonant states [32,33]. The angular dependence is strong evidence that this effect is not due to quantum size effects in the electrodes [34]. A similar negative dMR region in $Co_2MnSi/MgO/CoFe$ tunnel junctions was recently interpreted as an energy gap in the Co_2MnSi minority-spin band [35], but this explanation does not apply to our case because no such gap is expected for NiFe. While it is not possible to rule out unknown density of states effects, dynamic resonant tunneling is the most convincing origin because of its simplicity and ability to reproduce numerous experimental features from different MTJs with different materials.

In summary, novel bias-dependent oscillations were observed in the differential resistances of metal-insulator-metal (CoFeB/MgO/NiFe) tunnel junctions. These long sought oscillations are due to dynamic resonant tunneling mediated by interference of electrons that tunnel into the conduction band of the insulator (MgO). A coherent tunneling model using the exact solution of the Schrödinger equation and free electrons representing the electrodes qualitatively reproduced the bias dependence. The tunability of this newly demonstrated phenomenon, as well as its spin dependence, may help advance the development of tunable resonant tunneling systems for fundamental spintronics physics and applications.

Supported by the US DOE, the Swedish Foundation for Strategic Research, The Swedish Research Council, and The Göran Gustafsson Foundation. The authors thank J. M. Rowell, R. C. Dynes, H. Suhl, L. J. Sham, H. Dery, and L. Cywinski for useful discussions, and D. Mix for help with the wafer level measurements.

*Permanent address: Physics Department, University of South Florida, Tampa, FL 33620, USA.
†Present address: Center for Nanoscale Systems, Cornell University, Ithaca, NY 14853, USA.

[1] J. R. Oppenheimer, Phys. Rev. **31**, 66 (1928).
[2] L. Esaki, Phys. Rev. **109**, 603 (1958).
[3] I. Giaever, Phys. Rev. Lett. **5**, 147 (1960).
[4] B. D. Josephson, Phys. Lett. **1**, 251 (1962).
[5] G. Binnig *et al.*, Appl. Phys. Lett. **40**, 178 (1982).
[6] K. H. Gundlach, Solid-State Electron. **9**, 949 (1966).
[7] R. W. Dave *et al.*, IEEE Trans. Magn. **42**, 1935 (2006).
[8] J. J. Åkerman *et al.*, Europhys. Lett. **63**, 104 (2003).
[9] J. J. Åkerman *et al.*, Appl. Phys. Lett. **79**, 3104 (2001).
[10] J. J. Åkerman *et al.*, J. Magn. Magn. Mater. **240**, 86 (2002).
[11] W. F. Brinkman, R. C. Dynes, and J. M. Rowell, J. Appl. Phys. **41**, 1915 (1970).
[12] R. H. Fowler and L. Nordheim, Proc. Roy. Soc. London, Ser. A **119**, 173 (1928).
[13] J. Maserjian, J. Vac. Sci. Technol. **11**, 996 (1974).
[14] R. S. Becker, J. A. Golovchenko, and B. S. Swartzentruber, Phys. Rev. Lett. **55**, 987 (1985).
[15] M. B. Stearns, J. Magn. Magn. Mater. **5**, 167 (1977).
[16] W. H. Butler *et al.*, J. Appl. Phys. **85**, 5834 (1999).
[17] S. O. Valenzuela *et al.*, Phys. Rev. Lett. **94**, 196601 (2005).
[18] D. J. BenDaniel and C. B. Duke, Phys. Rev. **152**, 683 (1966).
[19] A. H. Davis and J. M. MacLaren, J. Appl. Phys. **87**, 5224 (2000).
[20] W. H. Butler *et al.*, Phys. Rev. B **63**, 054416 (2001).
[21] R. Wang *et al.*, Appl. Phys. Lett. **86**, 052901 (2005).
[22] D. J. Monsma and S. S. P. Parkin, Appl. Phys. Lett. **77**, 720 (2000).
[23] X. H. Xiang *et al.*, Phys. Rev. B **66**, 174407 (2002).
[24] R. C. Dynes and J. P. Carbotte, Physica (Amsterdam) **55**, 462 (1971).
[25] J. Mathon and A. Umerski, Phys. Rev. B **60**, 1117 (1999).
[26] C. W. Miller *et al.*, Appl. Phys. Lett. **90**, 043513 (2007).
[27] C. W. Miller *et al.*, Phys. Rev. B **74**, 212404 (2006).
[28] R. K. Singh *et al.*, Appl. Phys. Lett. **89**, 042512 (2006).
[29] S. Yuasa, T. Nagahama, and Y. Suzuki, Science **297**, 234 (2002).
[30] D. M. Roessler and W. C. Walker, Phys. Rev. **159**, 733 (1967).
[31] J. M. Rowell, in *Tunneling Phenomena in Solids*, edited by E. Burnstein and S. Lundqvuist (Plenum, New York, 1969), pp. 385–404.
[32] E. Y. Tsymbal *et al.*, Phys. Rev. Lett. **90**, 186602 (2003).
[33] E. Y. Tsymbal *et al.*, Prog. Mater. Sci. **52**, 401 (2007).
[34] R. C. Jaklevic *et al.*, Phys. Rev. Lett. **26**, 88 (1971).
[35] T. Ishikawa *et al.*, Appl. Phys. Lett. **89**, 192505 (2006).